

THE DERIVATION OF PHASE INTEGER AMBIGUITY FROM SINGLE INSAR PAIRS : IMPLICATIONS FOR DIFFERENTIAL INTERFEROMETRY

Andrew Sowter

IESSG, The University of Nottingham, University Park, Nottingham, NG7 2RD, UK.

Abstract

SAR Interferometry (InSAR) is a technique that is fast becoming an attractive prospect for routine derivation of land deformation parameters in events of a long-term and cataclysmic nature. The technique involves the analysis of the interferometric phase gradient, in both temporal and spatial dimensions, as it is generally difficult to derive the absolute value of the phase due to an integer ambiguity. Thus, InSAR methods are generally restricted to the measurement of deformation change from an arbitrary baseline rather than in the derivation of absolute position.

This paper describes a rigorous InSAR geometry based on a range-Doppler approach similar to that used in radargrammetry. An analysis of this geometry in the spaceborne case highlights the deficiency of the far-field approximation but also shows that a simple derivation of the phase integer ambiguity is possible from a single InSAR phase measurement. The accurate geolocation of wrapped phase values is then possible, limited only by the values of the pseudo-range contained in the image headers. Only very coarse ground control, if necessary at all, is needed to locate a full interferogram. The rigorous geometry presented is applicable to all airborne and spaceborne configurations and the generalised position vector may be transformed to height and position related to any reference datum and map projection through standard geodetic transformations.

The implications for Differential InSAR are highlighted. Principally, a reduced reliance on accurate third party Digital Terrain Models is possible, allowing greater automation and, for cataclysmic events, a much faster reaction time.

1. Introduction

SAR interferometry is, and continues to be, a technique of great interest in geophysical remote sensing. Over the last 10-15 years, InSAR has proved itself to be a major tool in the monitoring of land deformation at centimetric accuracies (Zebker et al, 1994), earthquakes (e.g. Massonet et al, 1993), volcanoes (e.g. Briole et al, 1997), ice sheets (e.g. Goldstein et al, 1993), landslides (e.g. Fruneau et al, 1996) and terrain subsidence (e.g. Massonet et al 1997).

In essence, the interferometric technique has many similarities with GNSS where precise motion requires the analysis of carrier phase. In InSAR, the receiver is also the transmitter, meaning that the phase is related to the two-way delay, complicated further by the scattering mechanism of the target. If the scattering mechanism is unchanged from a different receiver position, the signals are correlated and the difference in carrier phase between the two positions can be calculated.

Like GNSS, the resulting phase difference can only be determined modulo 2π leaving a problem in that an integer phase ambiguity remains. In GNSS, there have been several methods proposed for its solution (e.g. Abidin, 1994; Leick, 1994; Han and Rizos, 1997) and some of these have been directly applied to the InSAR problem (Hanssen et al, 2001) albeit using many, stacked, interferograms.

Sowter, 2003, has proposed a method for the determination of the phase ambiguity for single SAR interferograms that has clear repercussions for the use of InSAR for monitoring land movements. This paper contains a re-development of the differential InSAR concept assuming the phase ambiguity is known.

2. InSAR Geometry

The analysis contained in this part of the paper follows the conventions of Sowter, 2003, throughout.

Consider the imaging geometry of a two-pass InSAR system where the two antennas are at points P_1 and P_2 and are both imaging a target at T (Figure 1).

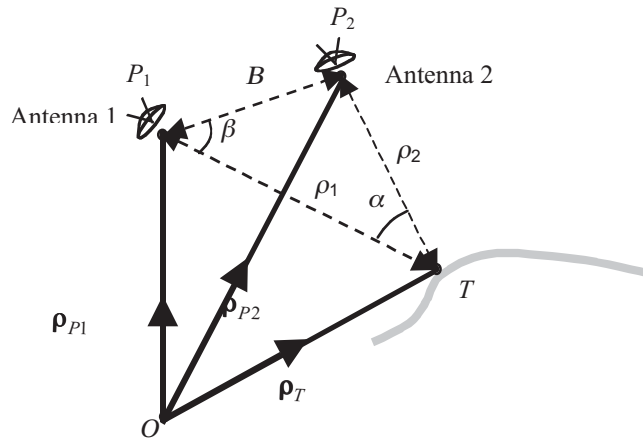


Figure 1. Typical InSAR Geometry

The full 3-d location of the target at T may be found by solving the three equations:

$$f_{D1} = -\frac{2}{\lambda|\boldsymbol{\rho}_T - \boldsymbol{\rho}_{P1}|} (\boldsymbol{\rho}_T - \boldsymbol{\rho}_{P1}) \cdot \mathbf{v}_{P1} \quad (1)$$

$$\rho_1 = |\boldsymbol{\rho}_T - \boldsymbol{\rho}_{P1}| \quad (2)$$

$$\frac{\lambda\phi}{4\pi} + \frac{\lambda}{2}\Delta n^{12} + \delta e = \frac{|\boldsymbol{\rho}_T - \boldsymbol{\rho}_{P1}|^2 - |\boldsymbol{\rho}_T - \boldsymbol{\rho}_{P2}|^2 + B^2}{2|\boldsymbol{\rho}_T - \boldsymbol{\rho}_{P1}|} \quad (3)$$

where f_{D1} is the Doppler frequency, λ is the radar wavelength, \mathbf{v}_{P1} is the satellite velocity vector at P_1 , ϕ is the interferometric phase, measured modulo 2π , Δn^{12} is the interferometric integer phase ambiguity and δe is the far field correction factor, given by:

$$\delta e = \frac{B^2 - (\rho_1 - \rho_2)^2}{2\rho_1} \quad (4)$$

Numerically, δe is very small compared to the Baseline and changes very little across an image. However, it is of the order of a wavelength and therefore cannot be ignored for precise applications that use the phase value. A good initial estimate for δe , applicable across the whole image, may be found through substitution of the pseudo-range values into equation 4.

The main problems with the solution of the above lie the identification of the integer phase ambiguity, Δn^{12} , the estimation of the range value, ρ_1 , and the value of the orbital baseline, B . A solution to this problem for single interferograms is given in Sowter, 2003.

To generate a digital surface model (DSM), the value of Δn^{12} is needed for all pixels across the whole interferogram, a not inconsiderable task if the ambiguity search process is applied everywhere. However, if Δn^{12} is determined for a single point and the phase is unwrapped from this solved point, any change in Δn^{12} would be compensated by the unwrapped value of ϕ . For areas isolated from a simple unwrapping procedure, such as those bounded by an impassable low coherent area, such as open water or dense forest, another control point needs to be found within the isolated area to form a start point for a second unwrapping process. Thus, the rigorous geolocation algorithm need not be applied across the whole image.

The range value ρ_1 cannot be simply related to the transmit-receive time (pseudo-range) as this will certainly be affected by tropospheric delay (Tarayre and Massonnet, 1996). However, the value used is within 10m of the actual value, assuming ERS-type errors (Sowter et al, 1990).

The orbital baseline has perhaps the most serious effect on the accuracy of InSAR (Li and Goldstein, 1990) and some baseline refinement is certainly required to meet most acceptable standards of precision (Zebker et al, 1994; Small, 1998).

For the following analysis it is assumed without loss of generality that the effects of errors has been minimised through baseline refinement, the selection of highly coherent targets and there being no change in atmospheric properties between acquisitions.

3. Phase Deviation

In an error-free differential interferometry scenario, an entirely feasible methodology would be to calculate the full 3-d positions of the same target in two interferograms and to examine its displacement. However, this impossible in the real world, mainly due to the pseudo-range approximation, and therefore it is usual to examine the interferometric phase change between the interferograms and to infer target motion from that value alone (Gabriel et al, 1989).

The interferometric phase is related to the baseline declination angle by:

$$\frac{4\pi}{\lambda} \cos \beta = \frac{1}{B} \left(\phi + 2\pi\Delta n^{ij} + \frac{4\pi}{\lambda} \delta e \right) \quad (5)$$

Consider a typical 3-pass InSAR configuration, where three SAR images are acquired in succession under the same atmospheric conditions, and that the three satellite positions and the target lie in the same plane (Figure 2). The wrapped interferometric phase between the first and second images and the first and third images are given by ϕ_{12} and ϕ_{13} respectively.

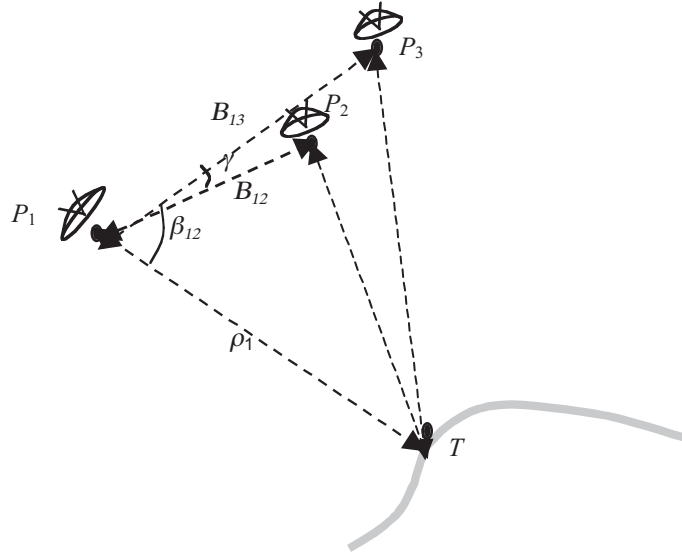


Figure 2. 3-Pass Differential InSAR Configuration.

The relationship between the two phase values and the two baseline declination angles are (equation 5):

$$\frac{4\pi}{\lambda} \cos \beta_{12} = \frac{1}{B_{12}} \left(\phi_{12} + 2\pi\Delta n^{12} + \frac{4\pi}{\lambda} \delta e_{12} \right) \quad (6)$$

$$\frac{4\pi}{\lambda} \cos(\beta_{12} + \gamma) = \frac{1}{B_{13}} \left(\phi_{13} + 2\pi\Delta n^{13} + \frac{4\pi}{\lambda} \delta e_{13} \right) \quad (7)$$

Differencing these two equations, it is found that:

$$\frac{8\pi \sin \frac{1}{2}\gamma}{\lambda} \sin \left(\beta_{12} + \frac{1}{2}\gamma \right) = \frac{1}{B_{12}} \left(\phi_{12} + 2\pi\Delta n^{12} + \frac{4\pi}{\lambda} \delta e_{12} \right) - \frac{1}{B_{13}} \left(\phi_{13} + 2\pi\Delta n^{13} + \frac{4\pi}{\lambda} \delta e_{13} \right) \quad (8)$$

The phase deviation, Φ , is defined by:

$$\Phi = \frac{1}{B_{12}} \left(\phi_{12} + 2\pi\Delta n^{12} + \frac{4\pi}{\lambda} \delta e_{12} \right) - \frac{1}{B_{13}} \left(\phi_{13} + 2\pi\Delta n^{13} + \frac{4\pi}{\lambda} \delta e_{13} \right) - \frac{8\pi \sin \frac{1}{2}\gamma}{\lambda} \sin \left(\beta_{12} + \frac{1}{2}\gamma \right) \quad (9)$$

which is zero when there has been no differential change.

4. Differential Interferometry using the Phase Deviation

An objective of differential InSAR is to calculate the phase deviation, Φ , for all pixels in the two interferograms. Any deviation from zero indicates an error or a change in one of the phase values, possibly indicating a change in target position at the third acquisition. If there has been a change in position, the range from P_3 to the target T will be shorter or longer than anticipated and therefore the phase value ϕ_{13} will be different from the anticipated value.

Now, let us consider that the target T has been displaced by a small amount between the second and third image acquisitions causing the phase to be given by:

$$\phi_{13} = \hat{\phi}_{13} + \delta\phi_{13} \quad (10)$$

This will cause a phase deviation of (equation 9):

$$\Phi = -\frac{\delta\phi_{13}}{B_{13}}$$

Note that it is not possible to fully estimate the direction or magnitude of the land motion that caused this effect as what is being detected in the change in the line of sight from P_3 only. The phase deviation then relates to a modification of the range from P_3 to T by an amount $\delta\rho_3$ given by:

$$\delta\rho_3 = -\frac{\lambda B_{13} \Phi}{4\pi} \quad (11)$$

It is common to resolve this into height δh and planimetric δr distortions such that:

$$\delta h = \frac{\lambda B_{13} \Phi}{4\pi} \cos \theta$$

$$\delta r = -\frac{\lambda B_{13} \Phi}{4\pi} \sin \theta$$

where θ is the incidence angle with the surface normal. The incidence angle can be calculated precisely using a surface normal vector and the vector from P_3 to T derived from equations 1-3.

This method outlined above is an extremely precise method for the derivation of the differential phase change. The assumptions are:

- The baseline is known very accurately;
- The phase must be unwrapped;
- Coarse ground control is available.

If all of these assumptions are satisfied, precise differential interferometry can be performed without recourse to using a DSM or using the far-field approximation.

5. Differential Interferometry using the Baseline Ratio

An alternative approach to differential InSAR without using a DSM is to use differences between flattened phases, scaled by the baseline ratio (Zebker et al, 1994). The interferometric phase is related to the baseline declination angle by equation 5. Consider that an estimate of the full phase, ϕ^* , derived from some 'flat earth' model, is given by:

$$\frac{4\pi}{\lambda} \cos \beta^* = \frac{1}{B} \left(\phi^* + 2\pi \Delta n^{*ij} + \frac{4\pi}{\lambda} \delta e^* \right)$$

The flattened phase, ϕ^{flat} , is obtained by subtracting the phase estimate from the full phase value:

$$\begin{aligned} \phi^{flat} &= \left(\phi + 2\pi \Delta n^{ij} + \frac{4\pi}{\lambda} \delta e \right) - \left(\phi^* + 2\pi \Delta n^{*ij} + \frac{4\pi}{\lambda} \delta e^* \right) \\ &= \phi - \phi^* + 2\pi (\Delta n^{ij} - \Delta n^{*ij}) + \frac{4\pi}{\lambda} (\delta e - \delta e^*) \\ &= \phi - \phi^* + K \end{aligned}$$

The purpose of the flattening is to minimise the value of K such that it is a small constant over the whole image, leaving only the local topographic component in ϕ^{flat} . This is assured by:

1. Making sure the flattening is as realistic as possible (e.g. it properly mimics the shape of the earth covered by the image footprint). It will also help to minimise the integer phase offset $\Delta n^{ij} - \Delta n^{*ij}$ if the flat earth model is coincident with the real topographic surface;
2. Unwrapping ϕ^{flat} . This will absorb the integer phase offset caused by the local topography.

Therefore:

$$\phi^{flat} = \frac{4\pi B}{\lambda} (\cos \beta - \cos \beta^*) \quad (13)$$

It is assumed that $\beta^* = \beta + \delta\beta$ for some small $\delta\beta$. Equation 13 thus becomes:

$$\phi^{flat} = \frac{4\pi B \sin \beta}{\lambda} \delta\beta$$

The value $B \sin \beta$ is the perpendicular component of the baseline, often termed B_{perp} or B_{\perp} . This value is assumed to be derivable from the orbit values, giving the baseline, and the sensor attitude parameters. Therefore, the flattened phase value becomes:

$$\phi^{flat} = \frac{4\pi}{\lambda} B_{\perp} \delta\beta$$

Considering the configuration of Figure 2, it is clear that:

$$\begin{aligned} \phi_{12}^{flat} &= \frac{4\pi}{\lambda} B_{\perp}^{12} \delta\beta \\ \phi_{13}^{flat} &= \frac{4\pi}{\lambda} B_{\perp}^{13} \delta\beta \end{aligned} \quad (14)$$

and therefore that the ratio between the flattened phases is given by:

$$\frac{\phi_{13}^{flat}}{\phi_{12}^{flat}} = \frac{B_{\perp}^{13}}{B_{\perp}^{12}} \quad (15)$$

A slight line-of-sight error from P_3 to T of an amount $\delta\rho_3$ will cause the interferometric phase to take a value of:

$$\phi_{13}^{flat} = \frac{4\pi}{\lambda} (B_{\perp}^{13} \delta\beta + \delta\rho_3)$$

Using equations 14 and 15 this becomes:

$$\phi_{13}^{flat} - \frac{B_{\perp}^{13}}{B_{\perp}^{12}} \phi_{12}^{flat} = \frac{4\pi}{\lambda} \delta\rho_3$$

This final expression allows the derivation of the line of sight error through a simple process of flattening, unwrapping, rescaling and differencing the phases. The assumptions in this second method are:

- The flat Earth model is sufficiently close to the topographic surface so that second order terms in $\delta\beta$ can be ignored and that phase integer ambiguities do not occur. This condition is more likely to be met in flat terrain, where the value of β will sweep monotonically from near to far range. In hilly terrain, β changes more rapidly over foreslopes than backslopes and therefore this condition is more likely to be in error.
- The phase must be unwrapped;
- The baseline is known very accurately; and
- The radar pointing angle is known very accurately. As this is related to the value of β , it, too, is a difficult value to ascertain over hilly terrain.

Satisfying all of these assumptions is an extremely tall order and therefore the method of differential InSAR that uses the phase deviation must be seen as the most appropriate for the derivation of precision products.

6. Conclusions

It has been demonstrated that differential SAR interferometry is possible without the use of a DSM, through the explicit derivation of the phase integer ambiguity using only coarse ground control. Furthermore, a method has been proposed to reduce the amount of ground control required by the implementation of any standard phase unwrapping scheme. The equations have been developed such that the far-field approximation is not adopted yet the equations governing the formation of the phase deviation and their interpretation hardly differ from those already in use. Therefore, it should be easy to implement such a scheme in any existing interferometric process.

The advantages of such a scheme are to free the user from the constraints formed by having to seek out a DSM where, for many parts of the world, accuracy, availability and resolution are an issue. Indeed, if the area in question has a coastline or a similar zero-elevation feature, the requirement for ground control disappears as a standard range-Doppler geocoding algorithm should be able to provide target location to a sufficient accuracy to seed the interferometric process across the image.

References

- Abidin, H.Z. (1994). On-the-fly ambiguity resolution. *GPS World*, 5(4), 40-50.
- Briole, P., D. Massonnet, and C. Delacourt (1997). Post-eruptive deformation associated with the 1986-87 and 1989 lava flows of Etna detected by radar interferometry, *Geophysical Research Letters*, 24(1), 37-40.
- Fruneau, B., J. Achache and C. Delacourt (1996). Observation and modelling of the Saint-Etienne de Tinee landslide using SAR interferometry. *Tectonophysics*, 265(3-4), 181-190.
- Gabriel, A.K., R.M. Goldstein, and H.A. Zebker (1989). Mapping Small Elevation Changes over Large Areas: Differential Radar Interferometry. *Journal of Geophysical Research*, 94(B7), 9183-9191.
- Goldstein, R., H. Engelhardt, B. Kamb and R. Frolich (1993). Satellite radar interferometry for monitoring ice sheet motion: Application to an Antarctic ice stream. *Science*, 262, 1525-1530.
- Han, S. and C. Rizos (1997). Comparing GPS ambiguity resolution techniques. *GPS World*, 8(10), 54-61.
- Hanssen, R.F., P.J.G. Teunissen and P. Joosten (2001). Phase Ambiguity Resolution for Stacked Radar Interferometric Data, *Proceedings of the International Symposium on Kinematic Systems in Geodesy, Geomatics and Navigation*, Banff, Canada, 5-8 June, 317-320.
- Leick, A. (1995). *GPS Satellite Surveying*, Second Edition, John Wiley & Sons, Inc. 584 pages.
- Li, F.K. and R.M. Goldstein (1990). Studies of multibaseline spaceborne interferometric synthetic aperture radars. *IEEE Transactions on Geoscience and Remote Sensing*, 28(1): 88-97.
- Massonnet, D., T. Holtzer and H. Vadon (1997). Land subsidence caused by the East Mesa geothermal field, California, observed using SAR interferometry. *Geophysical Research Letters*, 24(8), 901-904.
- Massonnet, D., M. Rossi, C. Carmona, F. Adragna, G. Peltzer, K. Feigl and T. Rabaut (1993). The displacement of the Landers earthquake mapped by radar interferometry. *Nature*, 364, 138-142.
- Small, D. (1998). Generation of Digital Elevation Models through Spaceborne SAR Interferometry. *Remote Sensing Series, Volume 30, Department of Geography, University of Zurich, Zurich, Switzerland*.
- Sowter, A. (2003). Phase Ambiguity Determination for the Positioning of Interferometric SAR Data. *Photogrammetric Record* (in press).
- Sowter, A., D.J. Smith, J.E. Laycock and H. Raggam (1990). An error budget for ERS-1 SAR imagery. *GEC-Marconi Research Centre Report under ESA Contract 7689/88/HE-I*.
- Tarayre, H. and D. Massonnet (1996). Atmospheric propagation heterogeneities revealed by ERS-1 interferometry. *Geophysical Research Letters*, 23(9), 989-992.
- Zebker, H.A., P.A. Rosen, R.M. Goldstein, A. Gabriel and C.L. Werner (1994). On the derivation of coseismic displacement fields using differential radar interferometry: The Landers earthquake. *Journal of Geophysical Research*, 99(B10): 19617-19634.
- Zebker, H.A., C.L. Werner, P.A. Rosen and S. Hensley (1994). Accuracy of topographic maps derived from ERS-1 interferometric radar. *IEEE Transactions on Geoscience and Remote Sensing*, 32(4): 823-836.